Catalysis Today 171 (2011) 97–103

Contents lists available at ScienceDirect

Catalysis Today

journal homepage: www.elsevier.com/locate/cattod

Syngas production from natural gas via catalytic partial oxidation using ceramic monolith catalyst at short contact time and elevated pressure

Shigeru Kado[a,*], Ken-ichi Imagawa[a], Asako Kiryu[a], Fuyuki Yagi[a], Takeshi Minami[a], Hironori Kawai[a], Ken-ichi Kawazuishi[a], Keiichi Tomishige[b,1], Arata Nakamura[c], Yoshifumi Suehiro[d]

[a] Chiyoda Corporation, Moriya-cho, Kanagawa-ku, Yokohama 221-0022, Japan
[b] Institute of Materials Science, University of Tsukuba, Tsukuba, Ibaraki 305-8573, Japan
[c] Inpex Corporation, Minato-ku, Tokyo 107-6332, Japan
[d] Japan Oil, Gas and Metals National Corporation, Chiba, Chiba 261-0025, Japan

ARTICLE INFO

Article history:
Received 31 October 2010
Received in revised form 21 February 2011
Accepted 2 March 2011
Available online 29 March 2011

Keywords:
Catalytic partial oxidation
High pressure
Short contact time
Monolith
Rh
Isotopic exchange

ABSTRACT

The development of the catalyst suitable for the catalytic partial oxidation (CPOX) of natural gas was investigated for the efficient production of synthesis gas. The catalyst of Rh/CeO_2 + ZrO_2 + MgO was found to show higher catalytic performance than Rh/MgO. The additional effect of CeO_2 and ZrO_2 to Rh/MgO on catalytic property was studied by H_2-TPR, isotopic oxygen exchange reaction and DRIFT spectroscopy. And it was revealed that the state of Rh can maintain metallic phase during the CPOX reaction, and that oxygen can be supplied from lattice oxygen, and that adsorbed CO can desorb easily. The application of foam monolith catalyst coated with developed support materials to high pressure and short contact time CPOX reaction has been investigated, and we have succeeded in demonstrating the stable catalytic performance for 2000 h at 1.0 MPa and 500,000 h^{-1} GHSV.

© 2011 Elsevier B.V. All rights reserved.

1. Introduction

Gas to Liquid (GTL) processes have received great attention as an effective technology for converting natural gas to ultra clean liquid fuels [1–3] as well as monetizing natural gas [4]. Evolution in Fisher–Tropsch reactor such as circulating fluid-bed reactor development by Sasol brought the growth in the capacity of FT process to tens of thousands of barrels per day of capacity [5]. In order to improve the total energy efficiency of GTL process, the syngas production reactor has been also developed because, in GTL process, the capital cost of syngas production section is considered to the largest portion of the total capital cost [6]. Also, the larger capacity of synthesis gas production section will be desired in order to reduce the capital cost per product [6]. Furthermore, the reduction of greenhouse gas, such as CO_2 emission, is strongly required for the suppression of the global warming. Therefore the development of more compact synthesis gas production processes with high energy efficiency is desired.

Chiyoda Corporation, University of Tsukuba, INPEX Corporation and JOGMEC (Japan Oil, Gas and Metals National Corporation) have jointly developed catalytic partial oxidation (CPOX, $CH_4 + 1/2O_2 \rightarrow CO + 2H_2$) catalyst and process to produce synthesis gas with higher efficiency and less natural gas consumption and CO_2 emission under high throughput conditions (GHSV = 1×10^5 to 1×10^6 h^{-1}). In the GTL process with larger capacity, the autothermal type reforming process is considered to be more economic than steam reformer [6].

As for the catalyst development, Green and co-workers have published that some noble metals like Ru, Rh, Ir could catalyze methane partial oxidation [7]. Hickman and Schmidt demonstrated the extremely short contact time reaction using Rh impregnated foam monolith catalyst and obtained very high syngas selectivity [8]. After this publication, there was a significant increase in publications from academia and industry. Some of them have already demonstrated the high pressure CPOX reaction [9–11] up to 2 MPa [12]. The higher operating pressure is desirable when considering the following synthetic process, such as FT process operated around 3 MPa. Basini et al. from Snamprogetti, energetically developed CPOX catalyst and processes by large scale, and published

---

[*] Corresponding author at: Research & Development Center, Chiyoda Corporation, 3-13, Moriya-cho, Kanagawa-ku, Yokohama 221-0022, Japan. Tel.: +81 45 441 9142; fax: +81 45 441 9728.
E-mail address: skado@ykh.chiyoda.co.jp (S. Kado).

[1] Present address: Tohoku University, School of Engineering, Aoba 6-6-07, Aramaki, Aoba-ku, Sendai, 980-8579, Japan.

0920-5861/$ – see front matter © 2011 Elsevier B.V. All rights reserved.
doi:10.1016/j.cattod.2011.03.009

many reports on both fundamental and practical study [13–16], as well as Shell, ConocoPhillips.

We have been also paid attention to CPOX reaction at short contact time and elevated pressure to reduce the reactor size and capital cost for syngas production drastically. Chiyoda Corporation and University of Tsukuba have studied the catalyst development, which is suitable for CPOX reaction from the viewpoints of Rh modification with other material mainly done by University of Tsukuba, and the effect of support material mainly done by Chiyoda Corporation. Tomishige and co-workers have found that the modification of Rh with Co or CeO_2 was effective to promote CPOX reaction and reduce the highest temperature of the catalyst bed. They also studied the structural characterization in detail and revealed that the strong interaction between Rh and additives [17–20].

On the other hand, Chiyoda Corporation has found that the addition of CeO_2 and ZrO_2 to Rh/MgO as support materials enhanced CPOX reaction [21,22]. The feature of this catalyst is described in this report including fundamental properties and application to the foam monolith catalyst, which is the candidate for the industrial catalyst due to the low pressure drop even at the high space velocity. The monolith foam catalyst has high surface to volume ratio, so that the homogeneous reaction such as complete oxidation at gas phase can be quenched. Surprisingly it is suggested from kinetic study that even over 2 MPa the heterogeneous reaction is still dominant over monolith foam catalyst [23]. But from the detailed chemistry and modeling based on experiments to know gas and solid temperature and mole fraction, mass transport limitation of oxygen is indicated due to the quite fast reaction rate [24]. This transport limitation means the difficulty of reactor design in scaling up, so the demonstration at practical conditions is quite important. We have succeeded in demonstrating the stable catalytic performance at 1.0 MPa and 500,000 h^{-1} GHSV using foam monolith catalyst.

2. Experimental

2.1. Catalyst preparation

A fundamental study such as the effect of support materials on catalytic performance at atmospheric pressure and each characterization was done using granule catalysts. The support material was prepared by physical mixing of each precursor of metal oxide such as CeO_2, ZrO_2 and MgO. The mixture was pressed into disk-shape to make tight contact among metal oxides and then calcined at high temperature. The sintered disk-shape support material was crushed and sieved into desired granule size from 0.36 to 0.43 mm before an aqueous solution of Rh precursor was impregnated by incipient wetness method. Finally, the catalyst was calcined again at moderate temperature after drying completely.

A stability test at high pressure and GHSV was examined over monolith catalyst employing α-Al_2O_3 ceramic foam as substructure. The disk-shape support material prepared by the same way described above was crushed into fine powder using ball mill to prepare water solvent slurry. The ceramic foam was coated with support material by slurry and calcined followed by Rh loading by incipient wetness method.

2.2. Catalytic performance

The catalytic performance at atmospheric pressure was evaluated using fixed bed flow type reactor whose schematic diagram has been already reported [21]. The thermowell for measuring the temperature by thermocouple was installed through the center of catalyst bed. The outlet temperature of the catalyst bed mentioned in the section of results was measured by this thermocouple.

Table 1
Composition of town gas used for catalyst stability test shown in Figs. 10 and 11.

Species	Volume %
CH_4	89
C_2H_6	6
C_3H_8	3
C_4H_{10}	2

The catalyst was reduced by hydrogen around 900 °C before catalytic performance test. After the reduction, the mixture of $CH_4/O_2/Ar = 30/15/55$ was introduced at atmospheric pressure and 400,000 h^{-1} GHSV. The catalyst bed was heated by external heating system for 3 h to confirm the steady state of the reaction, and then the electronic furnace outside the reactor was removed to achieve the autothermal condition.

The stability test at high pressure and GHSV was examined using another bench-scale reactor system by feeding compressed town gas whose contents are listed in Table 1, pure oxygen and steam at almost 1 N m^3/h total flow rate. In this case, the monolith catalyst was employed without thermowell put through the catalyst bed to avoid any possible heat loss. The standard conditions were 1.0 MPa, 500,000 h^{-1} GHSV, $O_2/C = 0.5$ and $H_2O/C = 0.04$–0.08. The experiments were conducted under autothermal condition.

Both reactor systems were equipped with on-line TCD-GC system to detect H_2, CO, CH_4 and CO_2. During every experiment shown in the section of results, no oxygen was detected.

2.3. Characterization

Hydrogen temperature programmed reduction (H_2-TPR) profile of the granule catalyst was measured by introducing 2.5% H_2 diluted with He with increasing temperature from ambient temperature to 850 °C. After the temperature reached 850 °C, it was maintained for 30 min until H_2 consumption was completed. Before H_2-TPR, the sample was pretreated in air for 30 min and then in Ar for 30 min at 500 °C to remove the impurities adsorbed on the surface.

Oxygen isotopic exchange reaction was conducted by pulse method injecting $CH_4/O_2 = 2$ mixture gas with 2.5 μmol/pulse at 900 °C by flowing He carrier gas at 1,000,000 h^{-1} GHSV corresponding flow rate. The loading amount of Rh existing in the pulse reactor was as small as 0.1 μmol, which was much smaller than injection amount, so that the catalytic reaction proceeded under this condition. Before the pulse reaction, the catalyst was pretreated by the continuous flow of $CH_4/{}^{16}O_2 = 4\%/2\%$ mixture diluted with helium at 900 °C for 1 h to confirm the steady state of CPOX reaction. The effluent gas was monitored by mass spectroscopy.

DRIFT spectra were recorded using Nicolet 6700 (Thermo Fischer Scientific) at a resolution of 4 cm^{-1} by collecting 120 scans in about 80 s. The monolith catalyst was crushed into powder and 30 mg of them was installed in the apparatus and reduced. In the case of CO adsorption, CO was introduced by pulse up to saturation. Desorption property of CO was measured by increasing temperature from ambient temperature to 500 °C, and spectra were recorded at every 50 °C interval. In the case of CPOX reaction, $CH_4/O_2 = 4\%/2\%$ mixture diluted with nitrogen was introduced at 500 cm^3/min at fixed temperature.

3. Results and discussion

3.1. Additive effect of CeO_2 and ZrO_2 to MgO as support materials

The Rh/MgO-based catalyst has been examined in terms of the suitability for CPOX reaction, and the additive effect of CeO_2 and

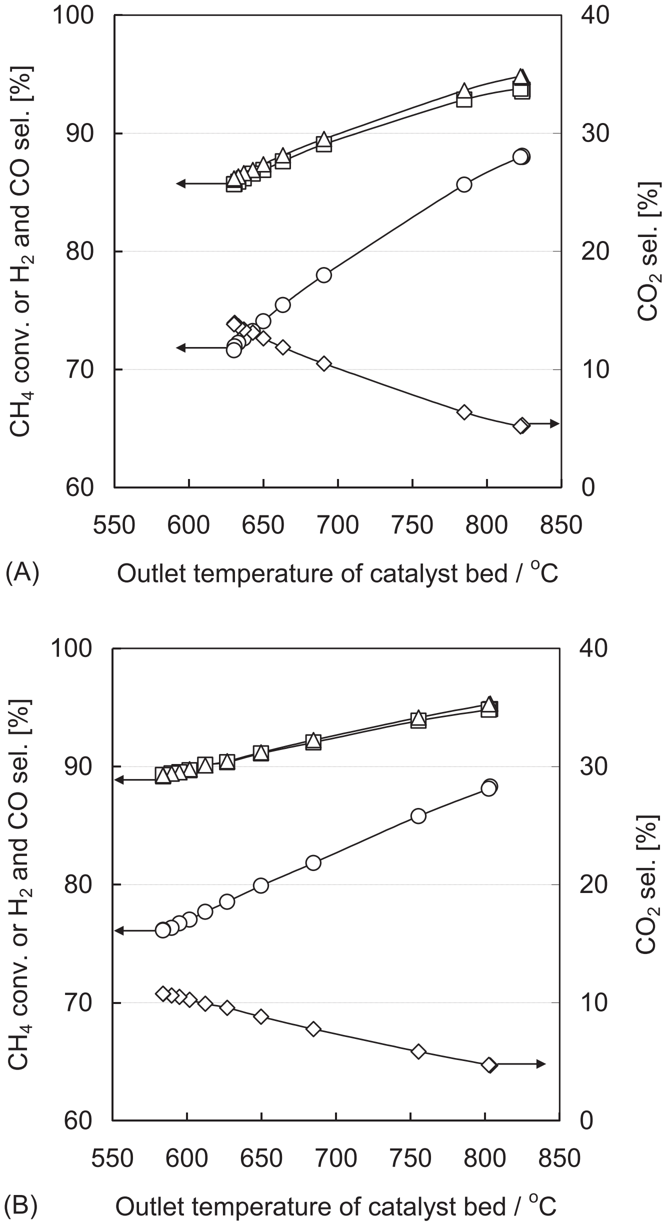

Fig. 1. Comparison of catalytic performance between Rh/MgO (A) and $Rh/CeO_2 + ZrO_2 + MgO$. (B) ○: CH_4 conversion, □ H_2 selectivity, △: CO selectivity, ◇: CO_2 selectivity. Reaction conditions: $CH_4/O_2/Ar = 30/15/55$, GHSV 400,000 h^{-1}, 0.1 MPa.

ZrO_2 to Rh/MgO was previously reported in detail [21]. Fig. 1 shows the behavior of methane conversion and selectivities to H_2, CO and CO_2 toward the outlet temperature of catalyst bed over Rh/MgO (A) and $Rh/CeO_2 + ZrO_2 + MgO$ (B) at atmospheric pressure. When the catalytic performance was compared at the same temperature, higher methane conversion and H_2 and CO selectivity and lower CO_2 selectivity were obtained over $Rh/CeO_2 + ZrO_2 + MgO$ rather than Rh/MgO. And the same catalytic performance could be achieved over $Rh/CeO_2 + ZrO_2 + MgO$ at lower temperature than over Rh/MgO. These results indicate that the addition of $CeO_2 + ZrO_2$ to Rh/MgO is effective to promote CPOX reaction.

When the outlet temperature was higher than 800 °C by the external heating system, the almost same methane conversion and selectivity were obtained over both catalysts. After the external heating system was removed, the outlet temperature began to decrease due to the autothermal condition and heat loss. Methane conversion and hydrogen selectivity also decreased, and CO_2 selectivity increased with the decrease in the temperature. Under the autothermal condition, the obvious effect of $CeO_2 + ZrO_2 + MgO$ support was observed to show higher methane conversion, H_2 and CO selectivity and lower CO_2 selectivity. Lower CO_2 selectivity indicates higher energy efficiency due to lower loss of valuable CO and lower exothermic heat derived from complete combustion. Owing to the higher CPOX performance, the outlet temperature finally reached 580 °C over $Rh/CeO_2 + ZrO_2 + MgO$, which was much lower than 630 °C over Rh/MgO.

Table 2
Deconvolution results of XPS spectra of catalysts after CPOX reaction shown in Fig. 1.

Catalyst	Contribution of Rh species (%)		
	Rh^0	Rh^{1+}	Rh^{3+}
Rh/MgO	0	85	15
$Rh/CeO_2 + ZrO_2 + MgO$	60	40	0

The addition of $CeO_2 + ZrO_2$ to Rh/MgO also affected the state of Rh particles during CPOX reaction. After the reaction shown in Fig. 1, the feed gas was quickly changed from $CH_4/O_2/Ar$ to Ar, and the catalyst was taken out from the reactor without exposure to the air as possible after the temperature decreased as low as room temperature. Then XPS measurement was done to know the state of the surface of Rh particles. By the deconvolution of XPS spectra, it is possible to know the contribution of Rh^0, Rh^{1+} and Rh^{3+}, and results are listed in Table 2. Over Rh/MgO, there was no contribution of Rh metal (Rh^0), and it was clear that the surface of Rh particles was partially oxidized during the reaction because the contribution of Rh^{1+} was as high as 85%. The addition of $CeO_2 + ZrO_2$ to Rh/MgO enabled Rh particles to maintain the metal state, and the contribution of Rh^0 reached as high as 60%. This high reducibility of Rh over $CeO_2 + ZrO_2 + MgO$ is thought one of the reasons why $Rh/CeO_2 + ZrO_2 + MgO$ showed higher performance than Rh/MgO.

Tomishige and co-workers have found that the modification of Rh with CeO_2 loaded on MgO promoted CPOX reaction. In their case, CeO_2 interacted with Rh directly, which was different from our catalyst where CeO_2 was added as a part of support material. They also investigated the oxidation degree of Rh particles during CPOX reaction by H_2 titration, and made it clear that high reducibility of Rh was important for the enhancement of CPOX reactivity [18]. This result is consistent with ours.

3.2. Contribution of lattice oxygen from support material over $Rh/CeO_2 + ZrO_2 + MgO$

The effect of CeO_2 and ZrO_2 addition to Rh/MgO on the contribution of oxygen pathway during the reaction was investigated. The comparison of H_2-TPR profiles between Rh/MgO and $Rh/CeO_2 + ZrO_2 + MgO$ were shown in Fig. 2. Over Rh/MgO, a small amount of hydrogen was consumed around 720 °C due to the reduction of Rh species, which is strongly interacted with MgO. Over $Rh/CeO_2 + ZrO_2 + MgO$, much larger amount of hydrogen was consumed than that of Rh/MgO due to the contribution of lattice oxygen derived from Ce–ZrO_x solid solution site around 470 °C and the partial reduction of CeO_2 from Ce^{4+} to Ce^{3+} around 800 °C. From the profile of $Rh/CeO_2 + ZrO_2 + MgO$, the reduction peak of Rh species could not be identified because the loading amount of Rh was quite small in this case and the contribution of lattice oxygen was too large.

In order to know the contribution of lattice oxygen to CPOX reaction, $^{16}O_2$ and $^{18}O_2$ isotopic exchange reaction was examined by pulse method at 900 °C and high flow rate of helium carrier gas corresponding to 1,000,000 h^{-1} GHSV. Before the pulse reaction, the catalyst was pretreated by the continuous flow of $CH_4/^{16}O_2$

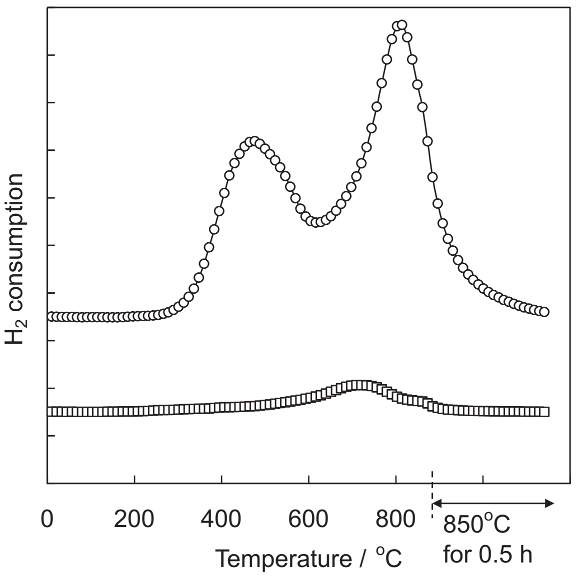

Fig. 2. H_2-TPR profile of Rh/MgO (□) and Rh/CeO_2 + ZrO_2 + MgO (○).

mixture diluted with helium at 900 °C for 1 h to confirm the steady state of CPOX reaction.

Fig. 3 shows the behavior of $C^{16}O$ and $C^{18}O$ composition in produced carbon monoxide monitored by mass spectroscopy when the pulse gas was varied from $CH_4/^{16}O_2$ to $CH_4/^{18}O_2$. As shown in Fig. 3(A), over Rh/MgO the main component became $C^{18}O$ at the same time as the feed oxygen was varied from $^{16}O_2$ to $^{18}O_2$. The reason why a small amount of $C^{16}O$ was still contained in the product after 10 pulses was the impurity of $^{16}O_2$ and moisture of $H_2{}^{16}O$ in $^{18}O_2$ cylinder. This result indicates that the oxygen contained in the products is derived from gas phase, and that there is no contribution of lattice oxygen to the reaction over Rh/MgO.

On the other hand, quite different result was obtained over Rh/CeO_2 + ZrO_2 + MgO as shown in Fig. 3(B). The main component in the produced carbon monoxide remained $C^{16}O$ even after the feed oxygen was changed from $^{16}O_2$ to $^{18}O_2$. It was surprising that the contribution of $^{18}O_2$ at the first pulse was only 6%. Conversely, most of oxygen was derived from lattice oxygen of support materials, not from gas phase. This fact indicates that oxygen exchange rate between gas phase and support materials was very rapid and faster than the surface reaction to produce carbon monoxide at 900 °C. In addition, as shown in Fig. 4, the pulse was injected 60 times until the composition of $C^{18}O$ reached 85%. At that time, the cumulative amount of $^{16}O_2$ contained in the produced CO, CO_2 and H_2O reached 20 μmol, which was quite larger amount than that of active oxygen or oxygen storage capacity of 1.25 μmol estimated from H_2-TPR shown in Fig. 2, but gradually approached to 23 μmol, which was the total oxygen amount existing in CeO_2 and ZrO_2. This means that the exchanged oxygen diffuses into the bulk of CeO_2 and ZrO_2 profoundly and rapidly.

After 60 pulses of $CH_4/^{18}O_2$, $CH_4/^{16}O_2$ mixture was injected by the same way. The behavior of $C^{16}O$ and $C^{18}O$ composition is also shown in Fig. 4. The same phenomenon of exchanging $C^{18}O$ to $C^{16}O$ was observed. Thus, the difference in oxygen pathway between Rh/MgO and Rh/CeO_2 + ZrO_2 + MgO is one of the reasons why Rh/CeO_2 + ZrO_2 + MgO showed higher CPOX performance.

3.3. Characterization by DRIFT method

In order to know another reason for higher performance of Rh/CeO_2 + ZrO_2 + MgO than the different oxygen pathway, DRIFT spectroscopic study was done for the state of adsorbed CO on the fresh surface and during CPOX reaction at 600 °C by feeding CH_4/O_2 diluted with 94% N_2. Over Rh/MgO, linear CO (2067 cm^{-1}) was observed on the fresh surface when saturated CO was fed at room temperature as shown in Fig. 5-spectrum (a). During CPOX reaction at 600 °C, the state of adsorbed CO was not varied so much and linear CO remained the main species as shown in Fig. 5-spectrum (b), except that the peak shifted from 2067 to 2015 cm^{-1} due to the lower coverage of CO on Rh surface than the saturate.

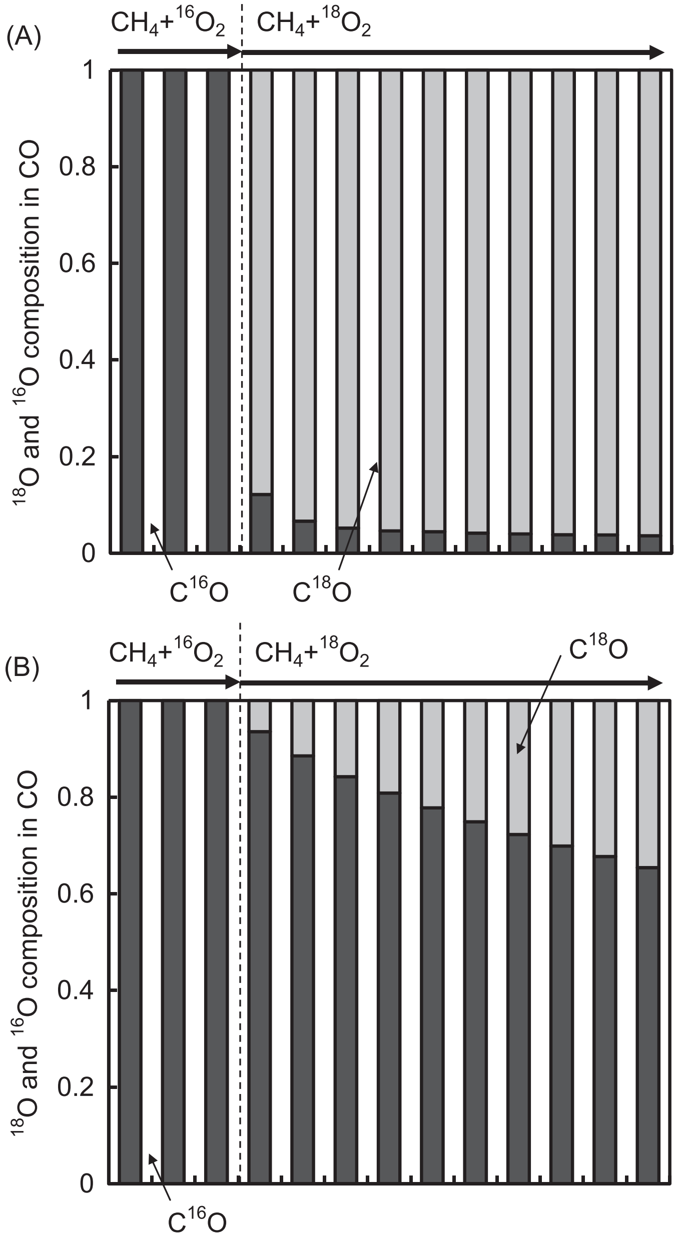

Fig. 3. $^{16}O_2/^{18}O_2$ isotopic exchange reaction over Rh/MgO (A) and Rh/CeO_2 + ZrO_2 + MgO. (B) By pulse reaction.

Over Rh/CeO_2 + ZrO_2 + MgO, the state of saturated CO adsorption was different from that of Rh/MgO. As shown in Fig. 6-spectrum (a), bridge CO (1905 and 1808 cm^{-1}) species were observed as well as linear CO (2044 cm^{-1}). The relatively large contribution of bridge CO over Rh/CeO_2 + ZrO_2 + MgO than Rh/MgO can be derived from the difference of morphology of Rh particles between them. TEM image of Rh/MgO used in this characterization has been previously reported by Tomishige and co-workers, and the average Rh particle size was estimated as small as 5.6 nm [19]. On the other hand, Rh

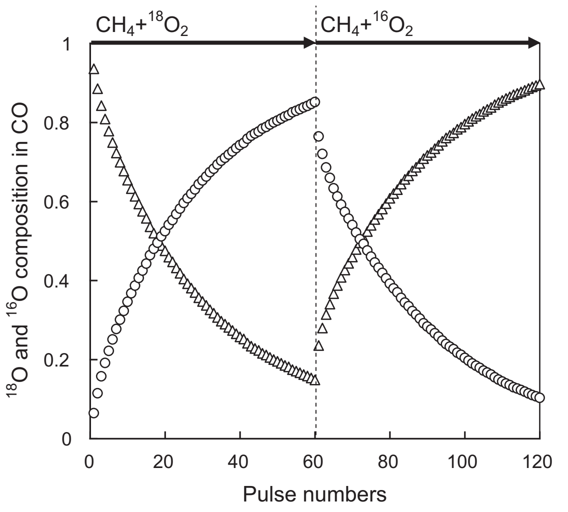

Fig. 4. Behavior of $C^{16}O$ (△) and $C^{18}O$ (○) composition in produced CO during $^{16}O_2/^{18}O_2$ exchange reaction over Rh/CeO_2 + ZrO_2 + MgO at 900 °C.

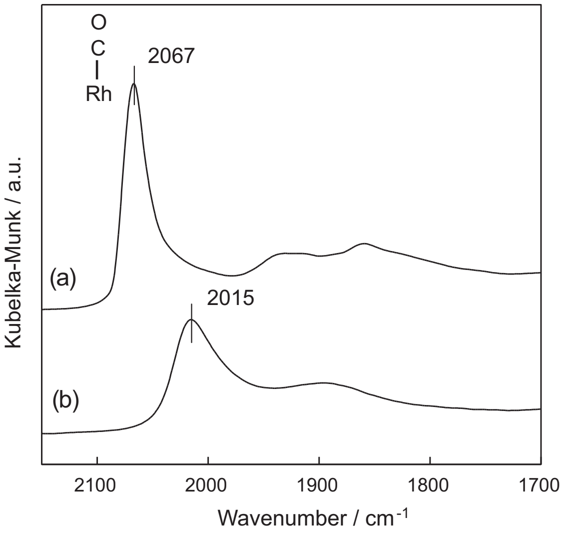

Fig. 5. DRIFT spectra of adsorbed CO over Rh/MgO on fresh surface after H_2 reduction (a), and during CPOX at 600 °C (b).

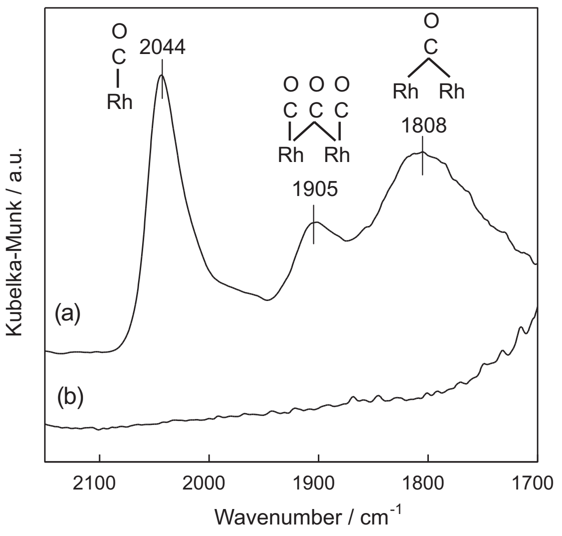

Fig. 6. DRIFT spectra of adsorbed CO over Rh/CeO_2 + ZrO_2 + MgO on fresh surface after H_2 reduction (a), and during CPOX at 600 °C (b).

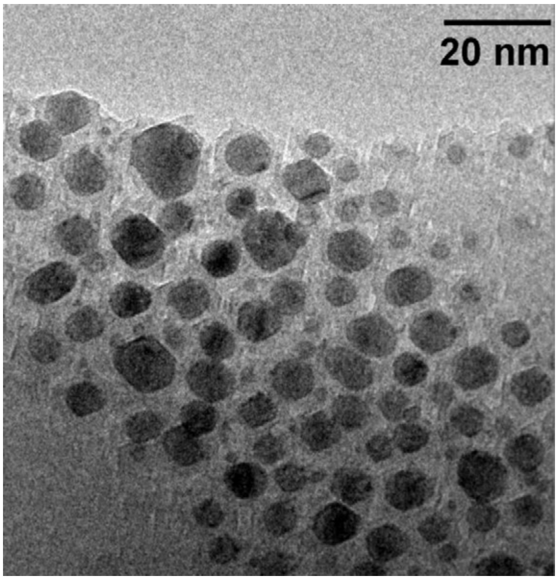

Fig. 7. TEM image of Rh/CeO_2 + ZrO_2 + MgO.

particle size over CeO_2 + ZrO_2 + MgO was as large as 10 nm, and Rh seemed to be crystallized as shown in Fig. 7. This variation in the morphology was derived from the difference in the condition for catalyst preparation.

The most interesting finding was that the peaks attributed to adsorbed CO disappeared during CPOX reaction at 600 °C over Rh/CeO_2 + ZrO_2 + MgO as shown in Fig. 6-spectrum (b). The difference between Fig. 5-spectrum (b) and Fig. 6-spectrum (b) is quite important to know the reason why Rh/CeO_2 + ZrO_2 + MgO shows higher catalytic performance for CPOX than Rh/MgO. Disappearance of adsorbed CO peaks during CPOX reaction over Rh/CeO_2 + ZrO_2 + MgO indicates two possibilities. One is the rapid desorption of CO from Rh surface as soon as CO is formed, the other is rapid oxidation of CO to CO_2.

In order to know the answer, CO desorption property was investigated over both catalysts by DRIFT method by increasing temperature from ambient temperature to 500 °C after the saturated CO adsorption. DRIFT spectra were measured at every 50 °C interval as shown in Fig. 8. Over Rh/MgO shown in Fig. 8(A), linear CO slightly decreased first, but bridge CO was stable until 200 °C. When the temperature was raised higher than 250 °C, both linear and bridge CO began to desorb drastically, and there was no CO signal observed at 400 °C. The reason why CO spectrum was observed at 600 °C during CPOX reaction shown in Fig. 5(b) is the re-adsorption of produced CO remained in gas phase.

The quite different behavior was observed over Rh/CeO_2 + ZrO_2 + MgO as shown in Fig. 8(B). The linear and bridge CO simultaneously began to desorb as soon as increasing temperature. Fig. 9 summarizes CO-TPD profile of Rh/MgO and Rh/CeO_2 + ZrO_2 + MgO estimated from the CO peak area measured by DRIFT spectra. The adsorbed CO over Rh/CeO_2 + ZrO_2 + MgO was obviously easier to desorb than that over Rh/MgO. Also, the gas composition of CO/CO_2 during CO-TPD was examined by separate experiment using mass spectrograph as detector by increasing temperature continuously. The ratio of CO/CO_2 in desorbed gas over Rh/CeO_2 + ZrO_2 + MgO was approximately 5–8 until 300 °C, indicating that CO desorption was dominant rather than CO oxidation.

From this result, it is concluded that the reason why no CO peak was observed over Rh/CeO_2 + ZrO_2 + MgO during CPOX reaction as shown in Fig. 6 is the rapid CO desorption property from the surface of Rh particles leading to the higher catalytic performance for CPOX.

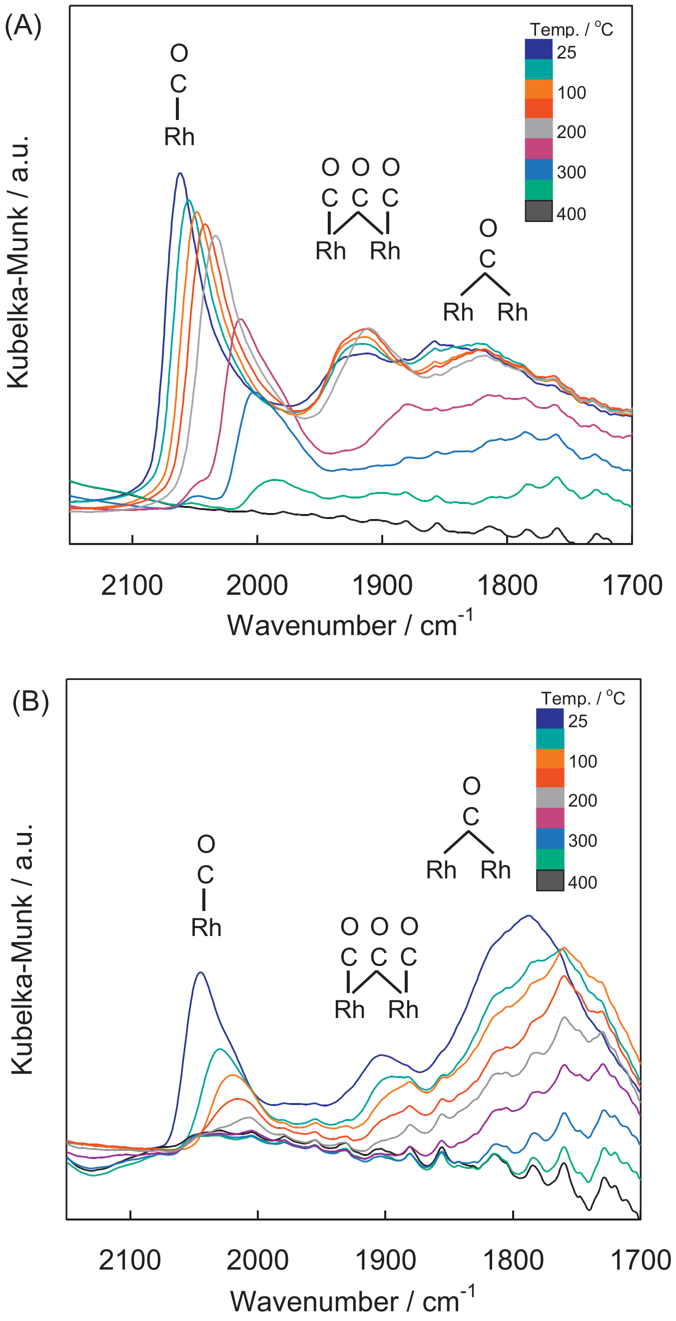

Fig. 8. Desorption property of adsorbed CO with temperature increase over Rh/MgO (A) and Rh/CeO_2 + ZrO_2 + MgO (B) observed by DRIFT.

3.4. Long term stability test of monolith catalyst at elevated pressure

The monolith catalyst was prepared by coating α-Al_2O_3 ceramic foam with Rh/CeO_2 + ZrO_2 + MgO catalyst uniformly. The stability test was conducted under the conditions of 1.0 MPa and 500,000 h^{-1} GHSV by feeding compressed town gas after desulfurization. The hydrocarbon contents of town gas are listed in Table 1. Pure oxygen was fed at the ratio of $O_2/C = 0.5$, and small amount of steam was added at the ratio of $H_2O/C = 0.04$.

The behavior of hydrocarbon conversion, hydrogen and carbon monoxide selectivities toward the time on stream was shown in Fig. 10 as well as that of H_2/CO ratio. At the initial activity hydrocarbon conversion reached 86% with 95% and 94% selectivities to hydrogen and carbon monoxide, respectively. The quite stable catalytic performance was demonstrated for 2000 h as shown in Fig. 10. Hydrocarbon conversion was almost stable and kept at 84.4% even after 2000 h. The selectivities and H_2/CO ratio were also very stable except the variation after 1140 h caused by the increase in H_2O/C ratio from 0.04 to 0.08. According to this increase in steam ratio, H_2/CO ratio in effluent gas varied from 1.85 to 1.88. After the long term test, there was no carbon deposition on catalyst surface.

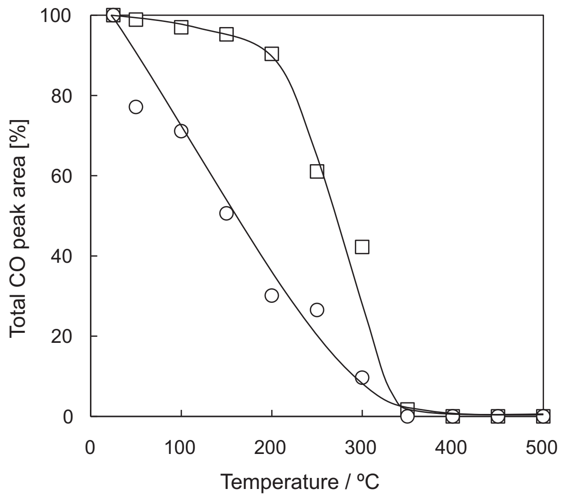

Fig. 9. Comparison of CO-TPD profile between Rh/MgO (□) and Rh/CeO_2 + ZrO_2 + MgO (○) estimated from variation of CO DRIFT spectra shown in Fig. 7.

Considering the synthesis process such as FT process and methanol process after the syngas production section, the ratio of H_2/CO ratio of 2 is desired. In the case of utilization of natural gas, it is necessary to adjust H_2/CO ratio in CPOX process because higher hydrocarbons with lower H/C than 4 are included in the feed gas as demonstrated in Fig. 10. The adjustment of H_2/CO ratio by increasing steam/carbon ratio in the feed gas was examined under conditions of 1.0 MPa, 750,000 h^{-1} GHSV and $O_2/C = 0.5$. The effect of steam/carbon ratio on H_2/CO ratio is shown in Fig. 11 with the behavior of hydrocarbon conversion. With the increase in the steam/carbon ratio, H_2/CO ratio increased due to the WGS reaction, and the ratio of $H_2/CO = 2$ was achieved when steam/carbon ratio was as high as 0.24. Interestingly, hydrocarbon conversion was not affected by steam/carbon ratio, suggesting that the contri-

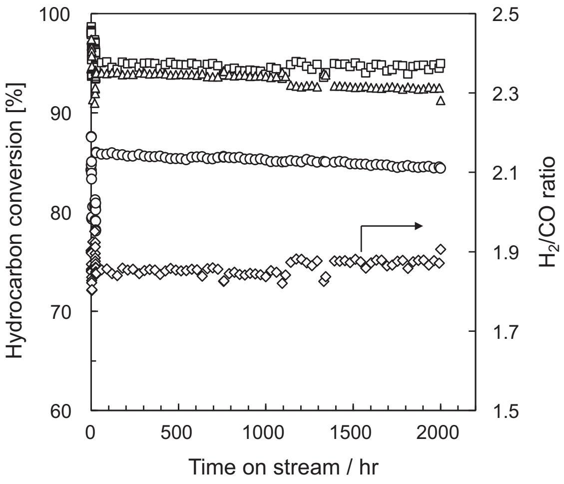

Fig. 10. Catalyst stability test for 2000 h using ceramic monolith catalyst coated with Rh/CeO_2 + ZrO_2 + MgO. Conversion (○), H_2 selectivity (□), CO selectivity (△), H_2/CO ratio (◇). Reaction conditions: 1.0 MPa, 500,000 h^{-1} GHSV, $O_2/C = 0.5$, $H_2O/C = 0.04$–0.08, feed hydrocarbon contents are listed in Table 1.

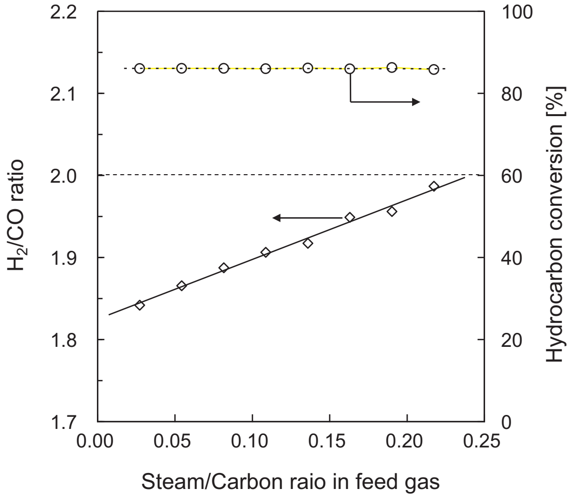

Fig. 11. Influence of steam/carbon ratio in feed gas on H_2/CO ratio and hydrocarbon conversion. H_2/CO ratio (◇), conversion (○). Reaction conditions: 1.0 MPa, 750,000 h^{-1} GHSV, O_2/C = 0.5, feed hydrocarbon contents are listed in Table 1.

bution of steam reforming reaction was not so large in this case. By other experiment, it was already confirmed that the increasing steam/carbon ratio did not affect the stability of the catalyst at least for 1000 h (data are not shown here).

4. Conclusions

The development of catalyst, which is suitable for CPOX of natural gas was studied focusing on the support material effect. It was found that the addition of CeO_2 and ZrO_2 to Rh/MgO enhanced the catalytic performance even at low temperature by maintaining Rh metal state during the reaction. The oxygen pathway over Rh/CeO_2 + ZrO_2 + MgO was thought quite different from that over Rh/MgO, and the contribution of lattice oxygen of support materials was revealed to play important role for production of carbon monoxide. Desorption property of CO was also quite unique to the developed catalyst. The adsorbed CO on Rh/CeO_2 + ZrO_2 + MgO was much easier to desorb than that on Rh/MgO, so that no adsorbed CO was observed by DRIFT during CPOX reaction.

Catalyst stability test was examined using the monolith catalyst, which was prepared by coating α-Al_2O_3 ceramic foam with Rh/CeO_2 + ZrO_2 + MgO at 1.0 MPa and 500,000 h^{-1} GHSV. The constant catalytic performance was demonstrated for 2000 h. The ratio of H_2/CO in the effluent gas could be adjusted by the steam/carbon ratio in the feed gas by controlling WGS reaction without affecting hydrocarbon conversion.

Acknowledgement

Financial support was provided by the Japan Oil, Gas and Metals National Corporation (JOGMEC) and is gratefully acknowledged.

References

[1] Y. Suehiro, J. Jpn. Inst. Energy 86 (4) (2007) 244.
[2] Y. Suehiro, Catal. Catal. 48 (4) (2006) 240.
[3] Y. Suehiro, J. Jpn. Inst. Energy 88 (8) (2009) 1017.
[4] A.P.E. York, Catal. Rev. 49 (4) (2007).
[5] C. Perego, R. Bortolo, R. Zennaro, Catal. Today 142 (2009) 9.
[6] D.J. Wilhelm, D.R. Simbeck, A.D. Karp, R.L. Dickenson, Fuel Process. Technol. 71 (2001) 139.
[7] A.T. Ashcroft, A.K. Cheetham, J.S. Foord, M.L.H. Green, C.P. Grey, A.J. Murrell, P.D.F. Vernon, Nature 344 (1990) 319.
[8] D.A. Hickman, L.D. Schmidt, Science 259 (1993) 343.
[9] A. Dietz, L.D. Schmidt, Catal. Lett. 33 (1995) 15.
[10] M. Lyubovsky, S. Roychoudhury, R. LaPierre, Catal. Lett. 99 (3/4) (2005) 113.
[11] A. Bitsch-Larsen, R. Horn, L.D. Schmidt, Appl. Catal. A: Gen. 348 (2008) 165.
[12] M. Fichtner, J. Mayer, D. Wolf, K. Schubert, Ind. Eng. Chem. Res. 40 (2001) 3475.
[13] L. Basini, A. Guarinoni, A. Aragno, J. Catal. 190 (2000) 284.
[14] L. Basini, K. Aasberg-Petersen, A. Guarinoni, M. Ostberg, Catal. Today 64 (2001) 9.
[15] M. Bizzi, L. Basini, G. Saracco, V. Specchia, Chem. Eng. J. 90 (2002) 97.
[16] L. Basini, Catal. Today 117 (2006) 384.
[17] S. Naito, H. Tanaka, S. Kado, T. Miyao, S. Naito, K. Okumura, K. Kunimori, K. Tomishige, J. Catal. 259 (2008) 138.
[18] H. Tanaka, R. Kaino, K. Okumura, T. Kizuka, K. Tomishige, J. Catal. 268 (2009) 1.
[19] H. Tanaka, R. Kaino, K. Okumura, T. Kizuka, Y. Nakagawa, K. Tomishige, Appl. Catal. A: Gen. 378 (2010) 175.
[20] H. Tanaka, R. Kaino, Y. Nakagawa, K. Tomishige, Appl. Catal. A: Gen. 378 (2010) 187.
[21] K. Imagawa, A. Nagumo, R. Kanai, T. Minami, K. Tomishige, Y. Suehiro, Stud. Surf. Sci. Catal. 167 (2007) 415.
[22] K. Imagawa, T. Minami, Petrotech 31 (4) (2008) 291.
[23] C.T. Goralski Jr., L.D. Schmidt, Chem. Eng. Sci. 54 (1999) 5791.
[24] D. Dalle Nogare, N.J. Degenstein, R. Horn, P. Canu, L.D. Schmidt, J. Catal. 258 (2008) 131.